2007

Benchmark study of run-to-run controllers for the lithographic control of the critical dimension

Mao, Ziqiang (John); Kang, Wei

Mao, J. & Kang, W. 2007, "Benchmark study of run-to-run controllers for the lithographic control of the critical dimension", Journal of Micro/Nanolithography, MEMS, and MOEMS, vol. 6, no. 2.
http://hdl.handle.net/10945/57022

Benchmark study of run-to-run controllers for the lithographic control of the critical dimension

Ziqiang (John) Mao
Intel Corporation
RNB-3-11
2200 Mission College Boulevard
Santa Clara, California 95120
E-mail: john.mao@intel.com

Wei Kang
Naval Postgraduate School
Department of Applied Mathematics
Monterey, California 93943

Abstract. We present a systematic robustness analysis for several feedback controllers used in photolithographic critical dimension (CD) control in semiconductor manufacturing. Our study includes several controllers based on either the exponentially weighted moving average (EWMA) estimation or Kalman filters. The robustness is characterized by two features, namely the controller's stability margin in the presence of model mismatch and the controller's sensitivity to unknown noise. Simulations on the closed-loop control system are shown for the performance comparison. Both the analysis and the simulations prove that the multiple-dimensional feedback controller developed in this paper using the average of previous inputs and outputs outperforms the other controllers in the group. [DOI: 10.1117/1.2743657]

Subject terms: feedback control; stability; sensitivity; critical dimension control; exponentially weighted moving average; Kalman filter.

Paper 06022RRR received Apr. 10, 2006; revised manuscript received Feb. 22, 2007; accepted for publication Mar. 2, 2007; published online Jun. 5, 2007. This paper is a revision of a paper presented at the SPIE conference on Metrology, Inspection, and Process Control for Microlithography XX, February 2006, San Jose, California. The paper presented there appears (unrefereed) in SPIE Proceedings Vol. 6152.

1 Introduction

The critical dimension (CD), a measurement of lines and ditches in the circuit, is a key parameter in characterizing the performance of semiconductor products. In a manufacturing process, improving the stability of the CD output results in yield improvement and cost reduction. It is known that the CD in a semiconductor product depends on the performance of exposure tools, in which the photolithography process takes place. These tools are equipped with onboard controllers that are able to monitor and adjust many parameters in the system. However, the dose and focus in the exposure tools are controlled by the users, typically a run-to-run controller. It is up to the process engineers to determine the best way of the control. A reliable controller of the dose and focus is essential in a manufacturing process to achieve stable run-to-run CD geometry. Several different types of feedback controllers are used by semiconductor manufacturers. In this paper, we introduce a systematic study on some of the representative run-to-run controllers. In addition, in this paper we introduce a feedback controller with a specially designed weighting method to achieve guaranteed stability and robustness.

This work is motivated by an Intel project of run-to-run controller design and implementation, which is a teamwork involving a group of process engineers, equipment engineers, and factory automation and controller designers across different organizations. Controller design and optimization is a key integral part in the entire project. Given the large volume of existing work on the run-to-run control, we found that a systematic method of controller analysis is a must-have for efficient validation and evaluation of the control algorithms to be implemented in manufacturing. As an integrated effort of run-to-run controller development, we must take into account the uncertainties and random noise in the process equipment. The goal of the paper is twofold: to analyze the robustness of several process controllers with model mismatch; and to introduce a process feedback controller for improved stability and robustness. This feedback controller is an output feedback controller of multiple dimensions with significantly improved stability and reduced sensitivity to unknown noise.

In Section 2, we present four existing feedback controllers. The first two feedback controllers are based on the estimation method of the EWMA (exponentially weighted moving average) and the d-EWMA (double EWMA), and the third one is a high-dimensional extension of the EWMA method. The fourth controller is based on the Kalman filter. In addition, a feedback controller of multiple dimensions is introduced that is proved to have better stability and robustness. In Section 3, state-space dynamical models of controlled processes are derived. The robustness study of the controlled processes is conducted based on these models. In Sections 4, we compare the stability of the four controllers under model mismatch. In Section 5, we compare the sensitivity of the four controllers under unknown noises. In Section 6, simulations are shown for the performance of the closed-loop system using all the controllers, and the results are consistent with the analysis and conclusions made in the previous sections.

2 Feedback Controllers

The run-to-run control of semiconductor manufacturing processes has been investigated by a number of researchers

1537-1646/2007/$25.00 © 2007 SPIE

from both universities and industrial research laboratories.[1–8] For instance, a process control system used by some semiconductor manufacturers was discussed in Refs. 17 and 18. The configuration tool for this system provides the user with the flexibility to define weighting parameters to optimize the performance of the controller. In Refs. 17 and 18 it was shown that equally weighting historical data can reduce the sensitivity to random noise. Another popular control algorithm is based on the EWMA algorithm, which uses exponential weighting factors. Some basics on EWMA can be found in the run-to-run control monograph.[19] Some typical applications of lithography APC can also be found in Ref. 15. In Ref. 21, the stability conditions and tuning guidelines are developed for multiple variable EWMA and double EWMA controllers with metrology delays.

In this section, we introduce some feedback controllers based on EWMA estimation that are widely used in the semiconductor industry for a variety of process steps. Then, in the next few sections, we use stability analysis and H_∞ control theory to analyze the robustness of these controllers. Let us assume a linear model defined by the following algebraic equations

$$y_t = au_t + c + w_t, \tag{1}$$

where y_t is the measured output from the tth run, u_t is the control input applied to the tth run, w_t is a random disturbance with zero mean and unknown distribution, a is the sensitivity from u_t to y_t, and c is a slowly varying parameter determined by other known or unknown factors. We call c the *intercept of the model*. A variety of processes in semiconductor manufacturing can be modeled in this way. The estimation of the value of both a and c is available using historical data from previous manufacturing activities or experimentation. However, an accurate value of the coefficients is not available due to equipment aging, the variation of wafer quality, and changes in the process environment. Thus, in the feedback control, estimated values of the coefficients are used. As a result, a feedback controller is always designed with a model mismatch. Such a model mismatch is an uncertainty in addition to the unknown noise in the process. Due to the complexity of the processes and the lack of physical models for semiconductor manufacturing equipment, the model mismatch can be relatively large. In this paper, we carry out a thorough performance analysis of feedback controllers in the presence of model mismatch. In addition to the model mismatch, the study also includes the unknown noise w_t, for which no *a priori* information such as the probability distribution or the covariance matrix is assumed. Following the literature of control engineering, a general linear output feedback control system has the following form:

$$\zeta_t = F\zeta_{t-1} + G\eta_{t-1},$$

$$u_t = C\zeta_{t-1}, \tag{2}$$

where u_t is the control input to be computed using the feedback law. In Eq. (2), u_t is determined by an intermediate variable ζ_t. The variable ζ_t follows the dynamics defined in Eq. (2), in which η_t represents the measured data from the process, and C, F, and G are constant matrices to be selected in the feedback design. In this paper, we defined η_t by the error of the process output, $y_t - y_T$. All the feedback control laws introduced in this section, except for the one using a Kalman filter, are presented in the unified form of the dynamical system in Eq. (2). The purpose of using this form is because of its convenience in the robustness analysis derived in the next two sections. However, we would like to emphasize that the quality of performance of a controller is determined by the way it is designed and implemented, but not by its formality. In addition, engineering knowledge from lithographic process engineers is indispensable in the effort of finding a good controller. This is the primary reason our research project was developed around real manufacturing data and the collaboration with process engineers.

Let $\bar{a}$ represent the estimation of a, a coefficient in Eq. (1). Then the factor of model mismatch is defined as follows:

$$\xi = \frac{a}{\bar{a}}.$$

It is used in this paper as a measure for the magnitude of the model mismatch. If $\xi = 1$ and if the value of c is known, then we have an ideal model that matches exactly with the true process. However, the performance of a controller designed based on the estimation $\bar{a}$ can be significantly downgraded if $\xi \neq 1$. In addition to the model mismatch, it is known that the value of the intercept, c, drifts during a real production process due to environmental changes and the system aging problem. Therefore, it is also critical to estimate the value of c for the purpose of feedback control. For the estimation of c, an EWMA method is defined as follows:

$$\bar{c}_t = \omega(y_t - au_t) + (1-\omega)\bar{c}_{t-1}, \tag{3}$$

where ω is a constant weight. If the variation of c follows the stochastic model of a first-order integrated moving average of a sequence of white noise, and if the weight in the stochastic model is known, then it can be proved that the EWMA estimation minimizes the mean squared error.[12] However, if the values of a and ω are not accurately known, then the EWMA estimation becomes inaccurate and even unstable. It is a known fact that under different controllers the impact of model mismatch on a control system or a manufacturing process is different. It is desired that a feedback controller can be designed to reduce the impact of the model mismatch in a process. The goal of this paper is to study the impact of the model mismatch for the photolithographic process under several feedback controllers, which are introduced in the rest of this section. We first introduce a feedback controller based on an EWMA estimation. Using $\bar{a}$, an estimation of a, the EWMA formula in Eq. (3) is revised as follows:

$$\bar{c}_t = \omega(y_t - \bar{a}u_t) + (1-\omega)\bar{c}_{t-1}. \tag{4}$$

A simple controller based on the EWMA estimation of c is a direct inverse of the estimated model

$$u_t = \frac{1}{\bar{a}}(y_T - \bar{c}_{t-1}),$$

where y_T is the target value of the process output. Substituting Eq. (4) into the feedback controller yields

$$u_t = \frac{1}{\bar{a}}(y_T - \omega(y_{t-1} - \bar{a}u_{t-1}) - (1-\omega)\bar{c}_{t-2}) = \frac{\omega}{\bar{a}}(y_T - (y_{t-1} - \bar{a}u_{t-1})) + \frac{1-\omega}{\bar{a}}(y_T - \bar{c}_{t-2}) = \omega u_{t-1} + \frac{\omega}{\bar{a}}(y_T - y_{t-1}) + (1-\omega)u_{t-1} = u_{t-1} - \frac{\omega}{\bar{a}}(y_{t-1} - y_T).$$

Thus, the feedback controller can be represented by the following dynamical system with model mismatch:

$$u_t = u_{t-1} - \frac{\omega}{\bar{a}}(y_{t-1} - y_T) = u_{t-1} - \frac{\omega\xi}{a}(y_{t-1} - y_T) \quad \text{(Controller I)}. \tag{5}$$

This formula is a special case of Eq. (2) in which $\zeta_t = u_t$, $\eta_t = y_t - y_T$, $F=1$, $G=-\omega/\bar{a}$, and $C=1$. Later, this formula is called the EWMA feedback controller and is referred to as Controller I. Under this controller, the control input at each run depends on the control input and the process output of the previous run. It is interesting to point out that the original model of the process is static. However, the closed-loop system under the feedback controller becomes dynamic in the sense that u_t is a function of u_{t-1}. For a dynamic system, issues such as stability, robustness, and sensitivity to noise become critical to the performance, as evidenced by the literature of robust control and H_∞ control.

In a real manufacturing process, an engineer may not trust the decision solely based on one previous measurement. A sequence of measurements can be used in the iterative formula. As a result, the dimension of the feedback controller becomes higher. The feedback controller can be written into the form of Eq. (2), with the following variables and matrices:

$$\zeta_t = u_t,$$

$$\eta_t = [y_t - y_T \; y_{t-1} - y_T \; \cdots \; y_{t-N} - y_T]^T,$$

$$F = 1,$$

$$G = -\frac{\omega}{\bar{a}}[\mathrm{w}_1 \; \mathrm{w}_2 \; \cdots \; \mathrm{w}_N],$$

$$C = 1, \tag{6}$$

where w_j, $j=1,2,\ldots,N$, are constant weights satisfying

$$\mathrm{w}_j > 0, \quad j = 1,2,\ldots,N,$$

$$\sum_{j=1}^{N} \mathrm{w}_j = 1. \tag{7}$$

In this paper, the following linear weights are used:

$$\frac{1}{1+2+\cdots+N}(N-j+1).$$

The selection of the weights depends on the performance of the process and the quality of the data. For a process with very slow autocorrelation, a short period of historical data can be used and an equal-weight schema like the one in Ref. 18 can be applied. To accommodate a relatively significant autocorrelation and noisy data, it is recommended to use more historical data and varying weights.

A controller defined by Eq. (6) is called an *extended EWMA controller* and referred to as Controller II. This controller is a simple extension of Controller I (EWMA). In fact, a compact iterative representation can be derived from Eq. (6). As a result, u_t equals u_{t-1} plus a correction term

$$-\frac{\omega}{\bar{a}}\sum_{j=1}^{N} \mathrm{w}_j(y_{t-j} - y_T),$$

which is the averaged error based on a sequence of previous runs. Controller II is considered in this paper because it is a more stable controller than the EWMA controller.

For systems with fast drift in the intercept, a *double EWMA* or *d-EWMA* method can be used to estimate both the intercept and its rate of change. Although an ordinary lithographic process has a slow intercept drift, under certain situations when the incoming thin-film thickness sensitivity is increased, the intercept drift could become faster. In this paper, we adopt the d-EWMA method from Ref. 13, which is different from some existing d-EWMA methods such as the one addressed in Ref. 10. Suppose the output follows the model

$$y_t = au_t + c + pt. \tag{8}$$

Given y_t and u_t, the intercept $c+pt$ and the drifting factor p are estimated by

$$\bar{d}_t = \omega_1(y_t - \bar{a}u_t) + (1-\omega_1)(\bar{d}_{t-1} + \bar{p}_{t-1}),$$

$$\bar{p}_t = \omega_2(y_t - \bar{a}u_t - \bar{d}_{t-1}) + (1-\omega_2)\bar{p}_{t-1}. \tag{9}$$

The feedback control is determined as follows:

$$u_t = \frac{1}{\bar{a}}(y_T - \bar{d}_{t-1} - \bar{p}_{t-1}).$$

Similar to the case of EWMA, the controller based on d-EWMA has an iterative formula defined by the following dynamics:

$$u_t = \frac{1}{\bar{a}}(y_T - \bar{d}_{t-1}) - \frac{\bar{p}_{t-1}}{\bar{a}} = \frac{1}{\bar{a}}(y_T - \omega_1(y_{t-1} - \bar{a}u_{t-1}) - (1-\omega_1) \times(\bar{d}_{t-2} + \bar{p}_{t-2})) - \frac{\bar{p}_{t-1}}{\bar{a}} = \frac{1}{\bar{a}}(y_T - \omega_1 y_{t-1} + \omega_1\bar{a}u_{t-1} - (1 - \omega_1)(y_T - \bar{a}u_{t-1})) - \frac{\bar{p}_{t-1}}{\bar{a}} = \frac{1}{\bar{a}}(\omega_1 y_T - \omega_1 y_{t-1} + \bar{a}u_{t-1}) - \frac{\bar{p}_{t-1}}{\bar{a}} = u_{t-1} - \frac{\omega_1}{\bar{a}}(y_{t-1} - y_T) - \frac{\bar{p}_{t-1}}{\bar{a}}.$$

To summarize, the iterative formula of the d-EWMA feedback controller is

$$u_t = u_{t-1} - \frac{\omega_1}{\bar{a}}(y_{t-1} - y_T) - \frac{\bar{p}_{t-1}}{\bar{a}} = u_{t-1} - \frac{\omega_1\xi}{a}(y_{t-1} - y_T) - \frac{\bar{p}_{t-1}\xi}{a}\ \text{(Controller III)}. \tag{10}$$

In the form of Eq. (2), we have

$$F = 1, \quad G = \left[-\frac{\omega_1}{\bar{a}}\frac{1}{\bar{a}}\right]^T, \quad C = 1,$$

$$\zeta_t = u_t, \quad \eta_t = [y_t - y_T\ \bar{p}_t]^T.$$

This is referred to as Controller III. All controllers introduced above have been used by semiconductor manufacturers for the run-to-run process control. Next, we introduce a feedback controller whose dynamics have multiple dimensions. In this feedback controller, it uses the average of both the control input and the process output variation from several previous runs. Although this controller can be written equivalently to the general form of some existing EWMA formula,[20] the following specially designed weighting method has two significant advantages: it improves the stability of the controlled system in the presence of significant model mismatch; and it reduces the impact of unknown disturbances in the system, which is very important for industrial manufacturing processes in which little is known about the process noise. These claims will be proved in the next few sections. The iterative formula of the feedback controller is defined as follows:

$$\zeta_t = [u_t\ u_{t-1}\ \dots\ u_{t-N+1}]^T,$$

$$\eta_t = [y_t - y_T\ y_{t-1} - y_T\ \cdots\ y_{t-N+1} - y_T]^T,$$

$$F = \begin{bmatrix} w_1 & w_2 & \cdots & w_{N-1} & w_N \\ 1 & 0 & \cdots & 0 & 0 \\ 0 & 1 & \cdots & 0 & 0 \\ \cdots & \cdots & \cdots & 0 & 0 \\ 0 & 0 & \cdots & 1 & 0 \end{bmatrix}_{N\times N} \quad \text{(Controller IV)},$$

$$G = -\frac{\omega}{\bar{a}}\begin{bmatrix} w_1 & w_2 & \cdots & w_N \\ 0 & 0 & \cdots & 0 \\ \cdots & \cdots & \ddots & \cdots \\ 0 & 0 & \cdots & 0 \end{bmatrix},$$

$$C = [1\ 0\ \cdots\ 0]. \tag{11}$$

In this paper, it is called Controller IV. Because it is designed based on the averaged control value of an EWMA controller, we also call it an *averaged EWMA controller*. Comparing to the extended EWMA, i.e., Controller II (extended EWMA), they both use the averaged output error, $\Sigma_{j=1}^{N}(\omega/\bar{a})w_j(y_{t-j}-y_T)$. However, the matrices, F in the two controllers are different to accommodate different η_t. The design in Controller IV (averaged EWMA) is able to reduce the impact of the unknown noise in the process. In fact, Controllers I, II, and IV are identical if $N=1$, i.e., we use the data from the most recent run only.

Before the end of this section, we introduce a controller based on a Kalman filter.[14] The advantage of this approach is to deal with both the system noise and the sensor noise in one framework, provided the covariance of the noise is known. The system is defined by

$$y_t = au_t + c_t.$$

Suppose the intercept term $c_t = y_t - au_t$ satisfies the IMA(0,1,1) model, $c_t = \bar{c}_{t-1} + v_{1t}, \bar{c}_t = \lambda c_t + (1-\lambda)\bar{c}_{t-1} = \bar{c}_{t-1} + \lambda v_{1t}$, where v_{1t} is a white sequence. Suppose y_t is measured with sensor noise. We define the system output by $z_t = y_t - au_t + v_{2t}$, where v_{2t} is the sensor noise. It is a white sequence having zero cross correlation with the sequence of v_{1t}. The dynamics are summarized as follows:

$$c_t = \bar{c}_{t-1} + v_{1t},$$

$$\bar{c}_t = \bar{c}_{t-1} + \lambda v_{1t},$$

$$z_t = y_t - au_t + v_{2t}. \tag{12}$$

Given z_t, we want to estimate $\bar{c}_t$ as the prediction of c_{t+1}. In the presence of system noise v_{1t} and the sensor noise v_{2t}, a Kalman filter is used to achieve an optimal estimation. Define

$$X = \begin{bmatrix} c_t \\ \bar{c}_t \end{bmatrix};$$

then the dynamical system (12) has the following form:

$$X_t = AX_{t-1} + Bv_{1t}, \quad A = \begin{bmatrix} 0 & 1 \\ 0 & 1 \end{bmatrix}, \quad B = \begin{bmatrix} 1 \\ \lambda \end{bmatrix},$$

$$z_t = CX_t + v_{2t}, \quad C = [1\ 0]. \tag{13}$$

Suppose the covariances of v_{1t} and v_{2t} are Q_t and R_t, respectively. Then the covariance matrix of Bv_{1t} is

$$\begin{bmatrix} 1 & \lambda \\ \lambda & \lambda^2 \end{bmatrix} Q_t.$$

Let $\hat{X}_0$ be the initial estimation of the initial state X_0. Let P_0 be the covariance matrix of X_0. Then the following Kalman filter provides an estimation $\hat{X}_t$,

$$\hat{X}_t = \hat{X}_t^- + K_t(z_t - C\hat{X}_t^-), \tag{14}$$

where

$$\hat{X}_t^- = A\hat{X}_{t-1}, \quad K_t = \frac{P_t^- C^T}{CP_t^- C^T + R_t},$$

$$P_t^- = AP_{t-1}A^T + \begin{bmatrix} 1 & \lambda \\ \lambda & \lambda^2 \end{bmatrix} Q_{t-1}, \quad P_t = (I - K_t C)P_t^-. \tag{15}$$

In feedback control, the estimation of $\bar{c}_t$, which is $[0\ 1]\hat{X}_t$, is used as the prediction of c_{t+1}. The control input for the tth. run is defined by

$$u_t = \frac{1}{a}(y_T - [0\ 1]\hat{X}_{t-1}). \tag{16}$$

The Kalman filter is introduced as an option of feedback design. However, it has fundamentally different structure and properties from the other controllers because the control gain of the closed-loop system is time-varying under the Kalman filter.

3 State-Space Dynamical Model of the Closed-Loop Systems

For the reason of robustness analysis and the application of H_∞ control theory, in this section we derive a state-space model for the controlled process. It is known that the state-space representation of a given system is not necessarily unique. The models in this paper are derived specifically for the purpose of study and analysis conducted in the sections that follow. Under Controller I (EWMA), we define the state variables of the process (1) by

$$X_t = \left[y_t - y_T \ \ u_t - \frac{y_T - c}{a} \right]^T. \tag{17}$$

Then, the dynamics of Eqs. (1)–(5) satisfies

$$X_t = \begin{bmatrix} -\omega\xi & a \\ -\dfrac{\omega\xi}{a} & 1 \end{bmatrix} X_{t-1} + \begin{bmatrix} w_t \\ 0 \end{bmatrix}. \tag{18}$$

Different from some existing analysis in the literature, the state variable defined by Eq. (17) is translated by

$$y_T, \ \frac{y_T - c}{a}.$$

If $X_t = [0\ 0]^T$ is a stable equilibrium of Eq. (18), then the translation defines the stable operating point of y_t and u_t. Similar translations are used for state-space analysis of other controllers in this paper.

For the d-EWMA analyzed in Castillo and Hurwitz.[10] a state-space model was derived. However, it is different from the d-EWMA in Chen and Guo,[13] which is adopted in this paper to define Controller III. Furthermore, the state-space model derived in this section has a transformation, which is able to provide important information about the equilibrium point of the controlled process. We define the state variable as follows:

$$X_t = \left[y_t - y_T \ \ u_t - \frac{y_T - (pt + c)}{a} \ \ \bar{p}_t - p \right]^T, \tag{19}$$

where $\bar{p}_t$ is the d-EWMA estimation denned by Eq. (9). Note that the meaning of stability in this case is different from the conventional definition. Due to the drift term pt, the controller has to drift accordingly to maintain y_t around a constant value. Therefore, the stability of the controlled process at $X_t = 0$ implies that the actual control input, u_t, drifts with the time-dependent function defined in the transformation used in Eq. (19),

$$\frac{y_T - (pt + c)}{a}.$$

In the state space, the dynamical equations of the controlled process (8)–(10) under Controller III (d-EWMA) have the following form [Eq. (20)]. Its derivation is omitted due to space limitations.

$$X_t = \begin{bmatrix} -\omega_1\xi & a & -\xi \\ -\dfrac{\omega_1\xi}{a} & 1 & -\dfrac{\xi}{a} \\ -\omega_1\omega_2\xi & \omega_2 a & 1 - \omega_2\xi \end{bmatrix} X_{t-1} + \begin{bmatrix} p(1-\xi) \\ \dfrac{p}{a}(1-\xi) \\ \omega_2 p(1-\xi) \end{bmatrix} + \begin{bmatrix} 1 \\ 0 \\ \omega_2 \end{bmatrix} \omega_t \tag{20}$$

The state-space models of the controlled process under Controller II (extended EWMA) or IV have higher dimension than that under Controller I (EWMA) and Controller III (d-EWMA). For Controller II, define the state variable as follows:

$$X_t = \left[u_t - \frac{y_T - c}{a} \ \ y_t - y_T \ \ y_{t-1} - y_T \ \cdots \ y_{t-N+1} - y_T \right]^T. \tag{21}$$

Then, the dynamical equation of the controlled process (1)–(6) is

$$X_t = \begin{bmatrix} 1 & -\frac{\omega\xi}{a}\beta_1 & -\frac{\omega\xi}{a}\beta_2 & \cdots & -\frac{\omega\xi}{a}\beta_{N-1} & -\frac{\omega\xi}{a}\beta_N \\ a & -\omega\xi\beta_1 & -\omega\xi\beta_2 & \cdots & -\omega\xi\beta_{N-1} & -\omega\xi\beta_N \\ 0 & 1 & 0 & \cdots & 0 & 0 \\ \vdots & \vdots & \vdots & \ddots & \vdots & \vdots \\ 0 & 0 & 0 & \cdots & 1 & 0 \end{bmatrix} X_{t-1} + \begin{bmatrix} 0 \\ 1 \\ 0 \\ \vdots \\ 0 \end{bmatrix}^T w_t. \tag{22}$$

Under Controller IV (averaged EWMA), the state variable is defined by

$$X_t = \left[y_t - y_T \; u_t - \frac{y_T - c}{a} \; y_{t-1} - y_T \; u_{t-1} - \frac{y_T - c}{a} \; \cdots \; y_{t-N+1} - y_T \; u_{t-N+1} - \frac{y_T - c}{a} \right]^T. \tag{23}$$

The dynamical equations in state space for the controlled process (1)–(11) has the following form:

$$X_t = \begin{bmatrix} -\omega\xi\beta_1 & a\beta_1 & -\omega\xi\beta_2 & a\beta_2 & \cdots & -\omega\xi\beta_{N-1} & a\beta_{N-1} & -\omega\xi\beta_N & \alpha\beta_N \\ -\frac{\omega\xi}{a}\beta_1 & \beta_1 & -\frac{\omega\xi}{a}\beta_2 & \beta_2 & \cdots & -\frac{\omega\xi}{a}\beta_{N-1} & \beta_{N-1} & -\frac{\omega\xi}{a}\beta_N & \beta_N \\ 1 & 0 & 0 & 0 & \cdots & 0 & 0 & 0 & 0 \\ 0 & 1 & 0 & 0 & \cdots & 0 & 0 & 0 & 0 \\ \vdots & \vdots & \vdots & \vdots & \ddots & \vdots & \vdots & \vdots & \vdots \\ 1 & 0 & 0 & 0 & \cdots & 0 & 1 & 0 & 0 \end{bmatrix} X_{t-1} + \begin{bmatrix} 1 \\ 0 \\ \vdots \\ 0 \end{bmatrix} w_t. \tag{24}$$

4 Robustness Analysis: Stability in the Presence of Model Mismatch

The robustness analysis conducted in this paper is twofold: the stability of the controlled process in the presence of model mismatch; and the sensitivity of the system to unknown disturbances. In this section, we focus on the stability of a controlled process under the controllers introduced in Section 2, using the dynamics model derived in Section 3. Due to the time-varying parameters in Kalman filters, it is not addressed in this section and the next section. However, the Kalman filter is included in the simulations shown in Section 6. It is well known that the stability of a dynamical system is determined by its eigenvalues, which are the roots of the characteristic equations defined by

$$\lambda I - \det(A) = 0,$$

where A is the matrix in the dynamical system, and I is the identity matrix. Under Controller I (EWMA), the controlled process [Eq. (18)] has the following characteristic equation:[16]

$$\lambda(\lambda - (1 - \omega\xi)) = 0. \tag{25}$$

Thus, the eigenvalues of the system are

$$\lambda = 0; \quad \lambda = 1 - \omega\xi.$$

For the system to be asymptotically stable, the absolute value of all eigenvalues must be less than 1. Therefore, the controlled process is stable if and only if

$$0 < \omega\xi < 2. \tag{26}$$

If the model mismatch defined by ξ is big enough so that $\omega\xi$ is out of the range $[0, 2]$, the system becomes unstable. As a result, the process drifts away exponentially by a small disturbance or perturbation in the system.

Given a controller, the range of $\omega\xi$ in which the system is kept stable is an important measure of the robustness of a controller. Because $\omega\xi$ is a common factor in all feedback controllers I–IV, we can directly compare the robustness of these controllers. In the following, we call $\omega\xi$ the *feedback gain ratio*.

For Controller III (d-EWMA), the characteristic equation of Eq. (20) is

$$\lambda(\lambda^2 + (\omega_1\xi + \omega_2\xi - 2)\lambda + (1 - \omega_1\xi)) = 0.$$

Therefore, the eigenvalues of the system in Eq. (20) are

$$\lambda = 0,$$

$$\lambda = \frac{1}{2}(2 - \xi(\omega_1 + \omega_2) \pm \sqrt{(2 - \xi(\omega_1 + \omega_2))^2 - 4(1 - \omega_1\xi)}). \tag{27}$$

Controller III (d-EWMA) is stable if and only if

$$|2 - \xi(\omega_1 + \omega_2) \pm \sqrt{(2 - \xi(\omega_1 + \omega_2))^2 - 4(1 - \omega_1\xi)}| < 2. \tag{28}$$

The stability under d-EWMA was addressed in Ref. 11. However, Eq. (27) is different from the one derived in Ref. 11 because the d-EWMA addressed here is the modified method from Ref. 13. In addition, the state-space model in Eq. (20) of the controlled process under Controller III (d-EWMA) is derived using the state variable [Eq. (19)], which contains a transformation. If a controller is stable, then the transformation provides the stable equilibrium. Note that a stable system is not necessarily stabilized at the desired equilibrium, especially when $p \neq 0$. In this case, the equilibrium of Eq. (20) under Controller III (d-EWMA) is moved by model mismatch. More specifically, let's assume zero noise $w_t = 0$. Suppose the model mismatch exists, i.e., $\xi \neq 1$. Then from the state variable defined by Eq. (19) and the dynamics defined by Eq. (20), the stable equilibrium is defined by

$$\begin{bmatrix} -\omega_1\xi & a & -\xi \\ -\frac{\omega_1\xi}{a} & 1 & -\frac{\xi}{a} \\ -\omega_1\omega_2\xi & \omega_2 a & 1-\omega_2\xi \end{bmatrix} X_{t-1} + \begin{bmatrix} p(1-\xi) \\ \frac{p}{a}(1-\xi) \\ \omega_2 p(1-\xi) \end{bmatrix} = 0.$$

If the system has drift $p \neq 0$, and model mismatch, $\xi \neq 1$, the equilibrium is not $X_t = 0$. Therefore, y_t is not necessarily stabilized at its desired value. However, in the case of $p = 0$, both Controller I (EWMA) and Controller III (d-EWMA) are able to stabilize the system at y_T in the presence of model mismatch, provided ξ satisfies Eq. (26) or (28).

Under Controller II (extended EWMA), the system has higher dimensions and the derivation of the characteristic polynomial becomes more involved. Thanks to the special structure of the matrix in Eq. (22), it is possible to derive the characteristic equation in an explicit form:

$$\lambda(\lambda^N + (\omega\xi\beta_1 - 1)\lambda^{N-1} + \omega\xi\beta_2\lambda^{N-1} + \cdots + \omega\xi\beta_N) = 0. \tag{29}$$

Its eigenvalues can be easily found by numerical computation. However, an explicit expression of eigenvalues is not available. A computational example is shown later in this section.

Controller IV (averaged EWMA) developed in this paper is a high-dimensional dynamics. The characteristic equation of Eq. (24) under Controller IV (averaged EWMA) consists of a higher-degree polynomial. Taking advantage of the triangular structure of the matrix in Eq. (24), we can derive the following characteristic equation:

$$\lambda^N(\lambda^N + (\omega\xi - 1)\beta_1\lambda^{N-1} + (\omega\xi - 1)\beta_2\lambda^{N-2} + \cdots + (\omega\xi - 1)\beta_N) = 0. \tag{30}$$

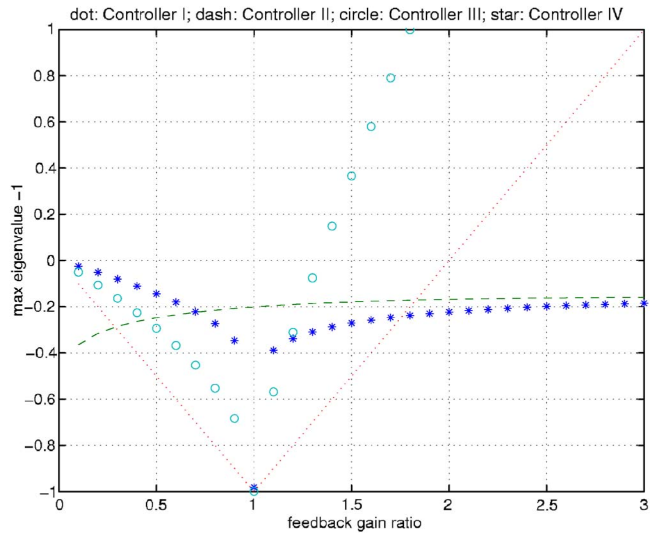

Fig. 1 Stability of controlled process.

For the purpose of the stability study, we use data from a manufacturing process to model the coefficients in Eq. (1). In the controllers, we assume inaccurate values of the coefficients to test the stability with model mismatch. In this case, $\xi \neq 1$. In Controllers I–IV, they all have a common term, $\omega\xi$, the feedback gain ratio. In the following, the eigenvalues of the controlled process are computed for the feedback gain ratio in the range of [0,3]. It is known that a linear system is asymptotically stable if and only if all eigenvalues lie in the unit disk of the complex plane, i.e., $|\lambda| < 1$ for all eigenvalues λ. The value of $\max\{|A|\} - 1$ for each controller is plotted in Fig. 1. If the value is less than zero, the controlled process under the feedback controller is asymptotically stable.

In this figure, the horizontal axis represents the value of the feedback gain ratio, $\omega\xi$, which is proportional to the model mismatch. The vertical axis represents the value of $|\lambda| - 1$, where only the eigenvalue with the largest absolute value is used. In the figure, the dotted curve is from the process under Controller I (EWMA). The curve is below zero when $\omega\xi$ is within the interval [0,2]. It implies that the controlled process under Controller I (EWMA) is stable for the value of $\omega\xi$ in this interval. It is a known result in the literature.[16] The star curve represents Controller IV (averaged EWMA). The dashed curve is Controller II (extended EWMA). Both have the largest interval of model mismatch in which the system is maintained stable. Actually, the controlled process under Controller IV (averaged EWMA) or II (extended EWMA) is stable for the feedback gain ratio to be as large as 12. The least robust controller is Controller III based on d-EWMA, which is represented by circles in the figure. The process becomes unstable when the feedback gain ratio is larger than 1.3. From Fig. 1, Controller IV (averaged EWMA) and controller II (extended EWMA)

Table 1 Stability robustness of controlled process.

Controller	Range of $\omega\xi$ for stability
Controller IV	$0<\omega\xi<12$
Controller II	$0<\omega\xi<12$
Controller I	$0<\omega\xi<2$
Controller III	$0<\omega\xi<1.3$

have the best stability robustness; Controller I (EWMA) has good stability robustness relative to Controller III (d-EWMA). The stability robustness is summarized in Table 1.

To directly compare the analysis in this section to the real data, a simulation is carried out. In the simulation, the model mismatch varies from 1 to as large as six times the value obtained from the real data. The root mean-square CD error of the controlled process is plotted together with the root mean-square CD error from the real data (see Fig. 2). The results show that Controller IV (averaged EWMA) has the best performance, which has a smaller error than the real data for a very large model mismatch. Controller II (extended EWMA) has bounded error. But the error is increased significantly when the model mismatch is larger than two times. Controller I (EWMA) becomes unstable for a large model mismatch. Controller III (d-EWMA) is unstable even for a small model mismatch. This result of the simulation is highly consistent with the analysis summarized in Table 1.

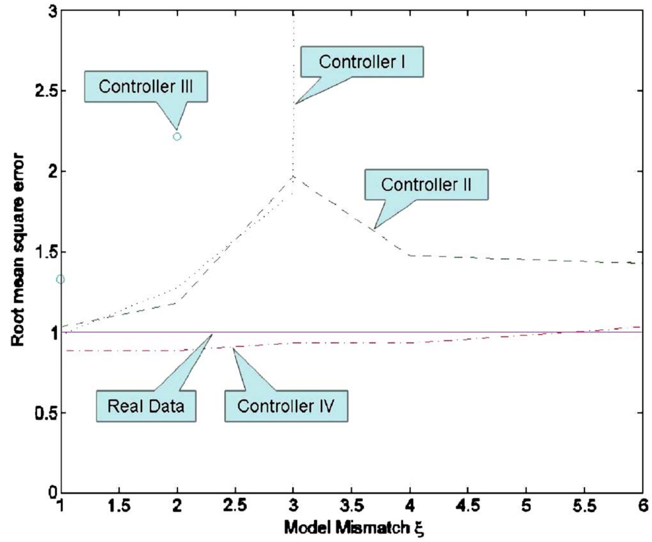

Fig. 2 Root mean-square CD error in controlled processes.

5 Robustness Analysis Sensitivity to Unknown Disturbances

We noted in the last section that the robustness study conducted in this paper consists of stability and sensitivity to unknown disturbances. The stability issue is addressed in the last section. Now, we focus our attention on the sensitivity issue. The analysis is conducted based on the H_∞ control theory. In semiconductor manufacturing, a large number of unknown disturbances and random noise with little or no *a priori* information make it extremely challenging to control a product output around its target value. Given two different controllers, and supposing both are stable, it is a known fact that the variation of the output measure of the process under one controller could be bigger or smaller than that under the other controller. The reason is that different controllers have different sensitivity to the disturbances in a process. Thus, stability is an important issue but not enough to fully characterize the performance of a controller. A goal of this section is to develop a method that quantitatively measures the sensitivity of feedback controllers. The method of analysis helps process engineers to select a better controller that is relatively less sensitive to unknown disturbances in a process so that the output of the product has smaller variation around its target value.

In this study, we treat the disturbance as an input for which we have no information about its probability distribution and covariance matrix. Thus, the analysis is especially useful when noise does not necessarily follow a statistical model, such as integrated moving average or white noise. The performance of a controller is measured by the error $y_t - y_T$. The sensitivity of unknown disturbance to the output error is measured by an H_∞ gain. In general, consider a linear dynamical system

$$x_t = Ax_{t-1} + Bw_t,$$

$$z_t = Cx_t, \tag{31}$$

where z_t is the output of the system, x_t is the state variable, and w_t is the unknown disturbance. In the case of a stable system and zero disturbance, $w_t=0$, the output of the system asymptotically approaches an equilibrium value. However, when $w_t \neq 0$, the value of z_t varies around the equilibrium point. For systems less sensitive to w_t, the variation is smaller. To measure the sensitivity of z to the disturbance w, we define its H_∞ gain. The H_∞ gain is less than or equal to a number γ if and only if

$$\sum_{t=1}^{n} \|z_t\|^2 \leq \gamma^2 \sum_{t=1}^{n} \|w_t\|^2$$

for an arbitrary input sequence $\{w_t\}$ and an arbitrary integer $n > 1$.[9] The lower bound of the gain can be defined using the transfer function in the following way:

$$\gamma = \max_{\omega}\{\bar{\sigma}(G^T(j\omega)G(j\omega))\}, \tag{32}$$

where $G(\cdot)$ represents the transfer function of Eq. (31), $\bar{\sigma}$ is the largest eigenvalue, and $j=\sqrt{-1}$.

For the process control of Eq. (1) under Controller I, II, III, or IV, the state-space equations of the controlled system are defined by Eqs. (18), (20), (22), and (24), respectively. From the state-space representation, the transfer functions can be calculated; then the H_∞ gain is computed. To reflect the sensitivity of the controlled process in the presence of model mismatch ($\xi \neq 1$), we compute the H_∞ gain for the gain ratio $\omega\xi$ within the range of [0,2], in which all con-

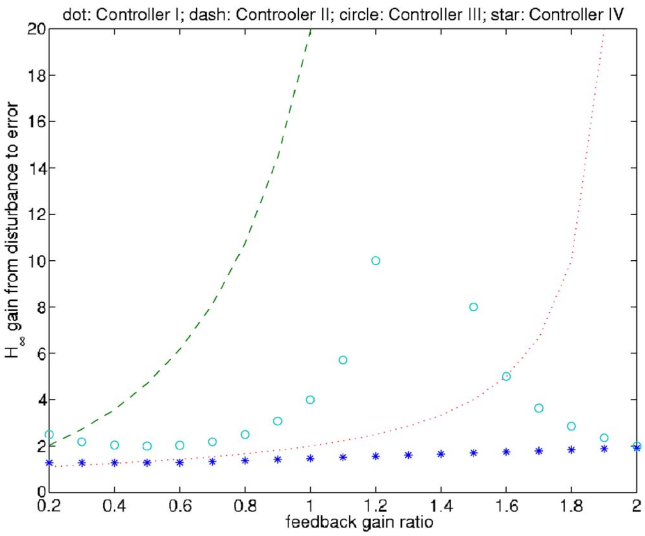

Fig. 3 H_∞ gain of controlled process.

trollers are stable except for Controller III (d-EWMA), which is stable in the interval [0,1.3]. The model used for computation is constructed based on data from a manufacturing process. The H_∞ gain of the controlled process under the four feedback controllers is shown in Fig. 3.

The horizontal axis in Fig. 3 represents the feedback gain ratio, $\omega\xi$, which is proportional to model mismatch. The vertical axis represents the H_∞ gain. In the figure, the dotted curve is the H_∞, gain under Controller I (EWMA). We use 2 as a reference level of the H_∞ gain. The curve of Controller I (EWMA) is below the level of 2 for the gain ratio in the interval of [0,1.2]. As the gain ratio exceeds 1.2, the H_∞ gain increases rapidly, which implies that a small disturbance results in a relatively big output variation. The most sensitive feedback controller is Controller II (extended EWMA), represented by the dashed curve. In this simulation, we chose $N=10$. The H_∞ gain of the controlled process under Controller II (extended EWMA) is around 2 for a small gain ratio and becomes much bigger when the gain ratio increases. Controller III (d-EWMA) has a reasonable H_∞ gain for $\omega\xi$ in the range of [0,0.8], which is about 2/3 of the interval of Controller I (EWMA). The controller with the smallest sensitivity is Controller IV (averaged EWMA), represented by the star curve. It is below 2 for the entire interval of $w\xi \in [0,2]$. Actually the H_∞ gain under Controller IV (averaged EWMA) is under 2 for $\omega t \in [2,2.4]$, which is three times the size of the interval of Controller III (d-EWMA) and twice that of Controller I (EWMA). The sensitivities of the controlled process under the four feedback controllers are summarized in Table 2.

From Table 2, it is interesting to observe that Controller II (extended EWMA) is the worst among the four controllers as far as the sensitivity to disturbances is concerned. However, it is one of the most stable controllers, as shown in the last section. It is a perfect example showing, that a performance analysis of a feedback controller should involve both stability and sensitivity to provide a comprehensive evaluation of the controlled process.

Table 2 H_∞ gain of controlled process.

Controller	H_∞ gain	Range of $\omega\xi$
Controller IV	$\gamma \leq 2$	[0.2.4]
Controller I	$\gamma \leq 2$	[0.1.2]
Controller III	$\gamma \sim 2$	[0.0.8]
Controller II	$\gamma \sim 2$	[0.0.2]

6 Simulations of Closed-Loop Systems

To further compare the performance of the controllers, we use a model based on the data from a manufacturing process. The data include multiple preventive maintenance (PM) events, rework lots, drift periods, irregular lot order, and metrology delay. In the simulation implementation, the metrology time and process time are synchronized to determine the lot order. In addition, deadband is used to keep the dose and focus constant when CD output is in a tight range of the CD target. Erroneous metrology readings are screened out. The calibration is also applied to data after each PM. For a direct comparison, we plot the simulation results together with the CD output of the real data. Simulations are carried out under Controllers I, II, III, IV, and the one based on a Kalman filter. The goal of the simulations is to evaluate the performance of the controllers in an environment with model mismatch, system drifts, and unknown noise. At first, the data from the manufacturing process are used to establish a linear model of the process. Then, we assume a model mismatch $\xi \neq 1$. In addition, we assume the model mismatch is not a constant. It changes at a rate called the *drifting factor*. To simulate the real environment, random noise is also added into the model. The root mean square of the random noise is determined from the real data. In Fig. 4, the rescaled root mean square of the CD error is shown. The simulations clearly show that the

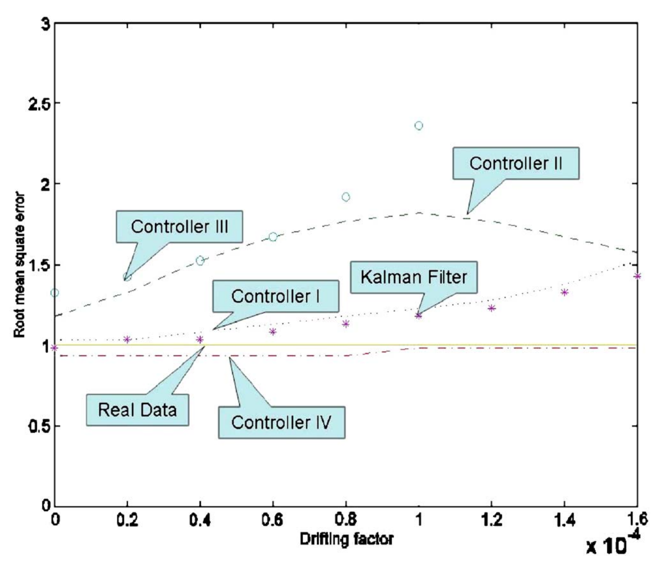

Fig. 4 Root mean square of CD error.

controller based on the Controller IV (averaged EWMA) has the smallest average error, which is consistently smaller than the averaged error computed from the real data. Under this controller, the root mean square of the error remains at almost a constant level while the rate of drift changes in a relatively large range. Relative to others, this controller is less sensitive to the model mismatch, drifts, and unknown noise. The controller based on the Kalman filter has the second-best performance. The performance of EWMA is similar to the Kalman filter-based controller. They both work well when the model mismatch is relatively small; and the error can be significantly enlarged in the case of a large model mismatch and fast drifting. The extended EWMA controller performs less satisfactorily relative to EWMA. It is interesting to note that the extended EWMA has a much larger stability region of model mismatch than that of EWMA. However, the extended EWMA controller is more sensitive to unknown noise. As a result, the extended EWMA performs less satisfactorily than EWMA. The d-EWMA controller is most sensitive to both the model mismatch and the random noise, although it has its advantage for systems with a linear drift assuming an accurate model.

7 Conclusion

The region of model mismatch and the H_∞ gain provide convenient tools for robustness study of feedback controllers. For the example analyzed, we found the averaged EWMA controller (Controller IV) has the best overall performance in terms of both robust stability and small sensitivity to unknown noise. The EWMA feedback controller (Controller I) is also reliable. The d-EWMA feedback controller (Controller III) is relatively less satisfactory. The extended EWMA controller (Controller II) is one of the most stable feedback controllers. However, it is relatively sensitive to unknown noise. In a simulation of closed-loop control, the Kalman filter-based controller performs similarly to the EWMA feedback controller. We would like to point out that the analysis method using model mismatch and H_∞ gain is not limited to the example in this paper. It is a general method of robustness analysis. The same idea is applicable to a large variety of process controllers of industrial manufacturing.

References

1. S. Adivikolanu and E. Zafiriou, "Extensions and performance/robustness tradeoffs of the EWMA run-to-run controller by using the internal model control structure," *IEEE Trans. Electron. Packag. Manuf.*, **23**, 56–68 (2000).
2. S. Adivikolanu and E. Zafiriou, "Robust run-to-run control for semiconductor manufacturing: an internal model control approach," *Proc. Am. Control Conf.* **6**, 3687–3691 (1998).
3. S. J. Baras and S. N. Patel, "Designing response surface model-based run-by-run controllers: a worst case approach," *IEEE Trans. Compon., Packag., Manuf. Technol., Part C* **19**(2), 98–104 (1996).
4. D. Boning, W. Moyne, and T. Smith, "Run by run control of chemical-mechanical polishing," 1995 IEEE/CPMT International Electronics Manufacturing Technology Symposium, pp. 81–87 (1995).
5. K. Chamness, G. Cherry, R. Good, and S. J. Qin, "A comparison of R2R control algorithms for the CMP with measurement delays," AEC/APC XIII Symposium (2001).
6. S. W. Butler, and J. Stefani, "Supervisory run-to-run control of polysilicon gate etching using in-situ ellipsometry," *IEEE Trans. Semicond. Manuf.* **7**, 193–201 (1994).
7. W. Campbell, "Model predictive run-to-run control of chemical mechanical planarization," PhD dissertation, The University of Texas at Austin (1999).
8. E. Del Castillo, and J. Y. Yeh, "An adaptive run-to-run optimizing controller for linear and nonlinear semiconductor processes," *IEEE Trans. Semicond. Manuf.* **11**(2) 285–295 (1998).
9. W. Lin and C. I. Byrnes, "H_∞-control of discrete-time nonlinear systems," *IEEE Trans. Autom. Control* **41**(4), 494–510 (1996).
10. E. Del Castillo and A. M. Hurwitz, "Run-to-run process control: literature review and extensions," *J. Quality Technol.* **29**, 184–196 (1957).
11. E. Del Castillo, "Long run and transient analysis of a double EWMA feedback controller," *IIE Trans.* **31**, 1157–1169 (1993).
12. G. Box, G. M. Jenkins, and G. C. Reinsel, *Time Series Analysis, Forecasting and Control*, 3rd ed., Prentice-Hall (1994).
13. A. Chen and R.-S. Guo, "Age-based double EWMA controller and its application to a CMP process," in *Run-to-Run Control in Semiconductor Manufacturing*, J. Moyne, E. del Castillo, and A. M. Hurwitz (eds.), CRC Press (2001).
14. A. Gelb, *Applied Optimal Estimation*, The MIT Press (l974).
15. C. P. Ausschnitt, B. Barker, W. A. Muth, M. Postiglione, and T. Walentosky, "Industrial strength lithography APC," *Proc. SPIE* **5044**, 1–11 (2003).
16. A. Ingolfsson and E. Sachs, "Stability and sensitivity of an EWMA controller," *J. Quality Technol.* **25**, 271–287 (1993).
17. D. W. Laidler, P. Leray, D. A. Crow, and K. E. Roberts, "Knowledge-based APC methodology for overlay control," *Proc. SPIE* **5044**, 32–43 (2003).
18. D. Crow, E. Joubert, A. Carlson, I. K. Abramovich, D. Karlikar, and M. Kish, "Enhancement of photolithographic performance by implementing and advanced process control system," *Proc. SPIE* **5378**, 192–203 (2004).
19. J. Moyne, E. Castillo, and A. M. Hurwitz, "*Run-to-Run Control in Semiconductor Manufacturing*," CRC Press (2001).
20. W. Muth, D. Crow, K. Roberts, and C. P. Ausschnitt. "CD control for high part count manufacturing line using CD normalization," AEC/APC Symposium, XVIII (2006).
21. S. J. Qin, G. Scheid, and T. Riley, "Adaptive run to run control and monitoring for a rapid thermal processor," *J. Vac. Sci. Technol. B* **21**(1), 301–310 (2003).

Ziqiang (John) Mao is currently a senior technologist and senior research scientist in Intel's Technology and Manufacturing Group. He has BS, MS, and PhD degrees in mathematics, computer science, and electrical engineering, respectively. He has published more than 40 papers in journals and conferences in the areas of lithographic advanced process control, multivariate statistical process control, fault detection and classification, multi-step cooperative process control, VLSI design, and robotics. He has been actively involved in the SPIE Microlithography conference, the AEC/APC Symposium, and ISMI conferences. He is a SPIE member and an IEEE senior member.

Wei Kang is currently a professor of applied mathematics at the U.S. Naval Postgraduate School. He received his BS degree in 1982 and MS degree in 1985 from Nankai University, China, both in mathematics. In 1991, he received his PhD degree in mathematics from the University of California at Davis. From 1991 to 1994, he was a visiting assistant professor of systems science and mathematics at Washington University in St. Louis. Dr. Kang received the Best Paper Award of the 6th International Conference on Control, Automation, Robotics and Vision held in Singapore in 2000. He was the 2003 recipient of the Carl E. and Jessie W. Menneken Faculty Award of the NPS Foundation. He was invited to give plenary speeches at several conferences organized by IFAC and SIAM. His research interests include PS methods of optimal control, nonlinear systems with bifurcations, normal forms and invariants, cooperative control of autonomous vehicles, industry applications of control theory, nonlinear filtering, and nonlinear H-infinity control. His early research includes topics on Lie groups, Lie algebras, and differential geometry.